Earth Surf. Dynam. Discuss., doi:10.5194/esurf-2016-33, 2016
Manuscript under review for journal Earth Surf. Dynam.
Published: 28 June 2016

Earth Surface Dynamics Discussions

Physical theory for near-bed turbulent particle-suspension capacity.

Joris T. Eggenhuisen[1], Matthieu J.B. Cartigny[2], Jan de Leeuw[1].

[1]Department of Earth Sciences, Utrecht University, Heidelberglaan 2, 3584 CS Utrecht, the Netherlands.
[2]National Oceanography Centre, Waterfront Campus, European Way, Southampton, SO14 3ZH, UK.

Correspondence to: Joris T. Eggenhuisen (j.t.eggenhuisen@uu.nl)

Abstract. The inability to capture the physics of solid-particle suspension in turbulent fluid flow is holding back application of multiphase computational fluid dynamics techniques to the many problems involving particle suspension in nature and society. We present a theory for particle suspension capacity near no-slip frictional boundaries of turbulent flows. The suspension capacity parameter Γ includes universal turbulent flow scales and material properties of the fluid and particles only. Comparison to measurements shows that Γ =1 gives the upper limit of observed suspended particle concentrations in a broad range of flume experiments and field settings. The condition of Γ >1 coincides with complete suppression of coherent turbulent structures near the boundary in Direct Numerical Simulations of sediment-laden turbulent flow. The theory outperforms previous empiric relations when compared to data. It can be applied as a concentration boundary condition in modelling studies of dispersion of particulates in environmental and man-made flows.

Keywords: Suspension capacity; turbulence; near-bed concentration; suspended sediment transport.

1 Introduction

Suspension of solid particles in turbulent fluid flow is one of the most widely occurring physical phenomena in nature, yet no physical theory predicts the particle suspension capacity of the wind, avalanches, pyroclastic flows, rivers, and estuarine or marine currents. Classic diffusion solutions for the distribution of suspended particles within turbulent flows [*Rouse*, 1937; *Vanoni*, 1940; *Montes Videla*, 1973; *McTigue*, 1981] do not predict the absolute particle concentration anywhere in the flow, but describe the relative concentration with respect to the concentration C_b near the boundary [mm's-cm]. The absolute sediment transport capacity of turbulent flows can therefore not be determined with a diffusion approach, and is in need of closure. Attempts to deduce capacity to suspend particles from turbulent stresses and buoyancy considerations [*Bagnold*, 1966; *Leeder*, 1983, 2007; *Leeder et al.*, 2005] have not solved the closure problem, and empiric formulations for near-boundary sediment suspension [*Smith and McLean*, 1977; *van Rijn*, 1984; *Garcia and Parker*, 1991, 1993; *Zyserman and Fredsoe*, 1994] have been widely used to close simulations of the particle concentration field. Here we establish a force-balance parameter Γ that compares turbulent forces near the boundary of a turbulent suspension to gravity and buoyancy forces acting on suspended particles. Comparison with data indicates that the theory predicts the absolute value of the near-boundary reference concentration C_b for Γ=1. Resolving the capacity of turbulent flows to suspend particles with a

Earth Surf. Dynam. Discuss., doi:10.5194/esurf-2016-33, 2016
Manuscript under review for journal Earth Surf. Dynam.
Published: 28 June 2016

concentration of C_b near the bed will allow determination of the sediment transport capacity of the entire flow when combined with classic turbulent diffusion approaches.

2 Theory for suspension capacity

2.1 Derivation Subsection

Suspended particles of density ρ_s with a volumetric sediment concentration C_b have a weight W per unit volume equal to

$$W = C_b \rho_s g\,, \qquad (1)$$

and experience an upward directed buoyancy force F_b equal to the weight of fluid displaced by particles

$$F_b = C_b \rho_f g\,. \qquad (2)$$

The resultant gravity force per unit volume is equal to

$$F_g = C_b\, g\left(\rho_s - \rho_f\right). \qquad (3)$$

The density of the solid particles typically exceeds the density of the fluid phase in transport of sediment particles on Earth's surface; so there F_g is directed downwards to the bed (Figure 1a).

Turbulence is widely quoted as a support mechanism for suspended particles. We postulate here that pressure and viscous forces exerted by turbulence onto suspended particles near the bed must average over time to supply a force F_{turb}, directed away from the bed and equal in magnitude to F_g, for sediment to be suspended with an equilibrium near-bed particle concentration C_b. The magnitude of F_{turb} will here be estimated from the scales of turbulent boundary layers. The basic idea that will be pursued is that observed accelerations of fluid parcels in turbulent flow are the expression of turbulent forces. Accelerations in wall-bound turbulence are at the front of current developments in unsteady turbulent fluid dynamics [*Yeo et al.*, 2010]. Physical experiments [*La Porta et al.*, 2001] and Direct Numerical Simulations (DNS) [*Vedula and Yeung*, 1999] investigating acceleration in homogenous isotropic turbulence have confirmed theoretical scaling of acceleration distributions proposed in the first half of the 20th century. However, near-boundary turbulence necessitates a more arduous analysis because the common neglect of the viscous term in the unsteady Navier-Stokes equation [*Vedula and Yeung*, 1999; *La Porta et al.*, 2001] does not hold close to the boundary [*Yeo et al.*, 2010]. Awaiting these more rigorous developments, we follow the idea proposed by Irmay [1960; *Bagnold*, 1966], to evaluate the average acceleration experienced by fictitious average fluid parcels representative of the multitude of underlying turbulent movements. Surprisingly, this average acceleration has the same sign for both downwards (negative) and upwards (positive) velocity excursions, resulting in a net upwards time-averaged acceleration which is not equal 0 m/s^2, despite the time average of turbulent velocity fluctuations being, by definition, equal to 0 m/s. In essence, this average upward acceleration is a result of the impermeability condition [*Stokes*, 1851; *Day*, 1990; *Pope*, 2000]. This condition necessitates that any upward directed turbulent motion must have been associated with an upward acceleration through time on a trajectory away from the boundary, where the vertical motion

Earth Surf. Dynam. Discuss., doi:10.5194/esurf-2016-33, 2016
Manuscript under review for journal Earth Surf. Dynam.
Published: 28 June 2016

must have been zero. Reversely, any downward directed turbulent motion of a fluid parcel moving towards the boundary must experience a similar upward acceleration to cancel the downward motion upon arrival on the boundary (Figure 1b). This simple approach enables the estimation of a force scale from the Newtonian inference that the upwards acceleration is the expression of a net upward turbulent force (F_{turb}) acting per unit volume of fluid. The magnitude of F_{turb} is now shown to follow from the scale-independent turbulence structure near a frictional boundary.

The velocity components (*u, v, w*) are directed along coordinate directions (*x,y,z*), and are here assigned to the stream-wise (*u*) and lateral (*v*) boundary-parallel velocities and the boundary-perpendicular velocity (*w*) respectively. The instantaneous, average, and turbulent velocity components are related as $(u,v,w)=(\overline{u},\overline{v},\overline{w})+(u',v',w')$, where the overbar denotes a time average, and the apostrophe denotes the instantaneous turbulent velocity fluctuation. The time average of turbulent velocity components is, by definition, 0, and measures of the average intensity of turbulence are conventionally reported either as the mean of squared turbulence $\overline{(u',v',w')^2}$, or as the root-mean-square of turbulence $\sqrt{\overline{(u',v',w')^2}}$ or simply $(u',v',w')_{RMS}$. Velocity near the frictional boundary is appropriately normalized with the friction velocity u^*: $(u^+,v^+,w^+)=(u,v,w)/u^*$ and distance along coordinates near the boundary are non-dimensionalized with friction velocity and kinematic viscosity ν, e.g.: $z^+=zu^*/\nu$. In this notation, the superscript $^+$ denotes non-dimensionalized velocity and length scales. The stream-wise velocity in turbulent shear flows collapses onto the "logarithmic law of the wall" for widely varying flow conditions under this normalization. This does not necessarily mean that the turbulence characteristics also collapse if normalized with the friction velocity. DeGraaff and Eaton [2000] note that such universal turbulence scaling is not supported by the body of available measurements. Townsend [1976] demonstrates, however, that similarity of turbulent motions is uniquely possible for the boundary-perpendicular component *w*, and not for the other components. This boundary perpendicular component has, indeed, been confirmed to collapse when normalized with the friction velocity (Figure 2; [*De Graaff and Eaton*, 2000]). The analysis presented here makes use of this collapse of $\overline{w'^2}^+(z^+)$, and its structure is therefore reviewed in detail.

The no-slip and impermeability conditions [*Stokes*, 1851; *Day*, 1990; *Pope*, 2000] require that fluid in contact with the boundary has no tangential or perpendicular velocity relative to the boundary. The boundary-perpendicular velocity component w^+ is therefore equal to 0 at $z^+=0$, and so is the turbulent component $\overline{w'^2}^+$. Immediately above a perfectly smooth boundary, at elevations of $z^+<<1$, molecular diffusion dominates over convection and velocity fluctuations exhibit Brownian motion [*Dreeben and Pope*, 1998]. In the viscous sublayer, further from the wall but below $z^+\sim5$, the stream-wise velocity increases as $u^+=z^+$. This is a region of two-component flow in x-y planes where boundary-parallel velocity fluctuations (u'^+,v'^+) start to be established but the vertical fluctuations remain small [*Pope*, 2000]. Fluctuations in the vertical

Earth Surf. Dynam. Discuss., doi:10.5194/esurf-2016-33, 2016
Manuscript under review for journal Earth Surf. Dynam.
Published: 28 June 2016

velocity component increase rapidly only above the viscous sublayer (~5<z^+). A peak value in the turbulence intensity is reached at a distance of $z^+_{Imax} \sim 90 \pm 10$ from the boundary, and it remains quasi constant throughout the near-boundary flow [*De Graaff and Eaton*, 2000]. In this analysis, we focus on the region of turbulent flow between ~5<z^+<~90 that exhibits strong vertical spatial gradients in average boundary-perpendicular velocity fluctuations (Figure 2).

Slightly different values for the maximum intensity of vertical turbulence are reported in literature. The peak value attained at the turbulence intensity maximum is $\overline{w'^2}(z_{Imax}) \sim 1.2u^{*2}$ or; $\overline{w'^2}^+(z^+_{Imax}) \sim 1.2$. Spalart [1988], Nezu & Nakagawa [1993], and Townsend [1976] report $w'^+_{RMS}(z^+_{Imax}) \sim 1.1$. Grass [1971] reports $w'^+_{RMS}(z^+_{Imax}) \sim 1.0$, and DeGraaff and Eaton [2000] report $\overline{w'^2}^+(z^+_{Imax}) \sim 1.35$. In this paper we use the numerical value of $\overline{w'^2}^+(z^+_{Imax}) \sim 1.2 \pm 0.1$.

Equations of motion for spatial variation in velocity under spatially varying acceleration have the form:

$$\tfrac{1}{2}v(x)^2 = \int a(x)dx \qquad (4)$$

Which can be written as

$$\tfrac{1}{2}\overline{w'^2}^+(z^+) = \int \overline{a}^+(z^+)dz^+ \qquad (5)$$

if applied to the average amplitude of the vertical turbulent motion.

Acceleration is non-dimensionalized with viscosity and friction velocity

$$a^+ = a\frac{\nu}{u^{*3}}, \qquad (6)$$

which follows naturally from the conventional non-dimensionalizations of z and (u,v,w) introduced above.

The acceleration is, a priori, assumed to have the functional form

$$\overline{a}^+(z^+) = C_1(90 - z^+)^2 \qquad (7)$$

Equation (7) is substituted in Eq. (5) and the integration is performed

$$\overline{w'^2}^+(z^+) = -\tfrac{2}{3}C_1(90 - z^+)^3 + C_2 \qquad (8)$$

The constants C_1 and C_2 are evaluated as $\frac{3}{2}\frac{1.2}{85^3}$ and 1.2 respectively from the boundary conditions of $\overline{w'^2}^+$ at z^+=5 and z^+=90, resulting in

Earth Surf. Dynam. Discuss., doi:10.5194/esurf-2016-33, 2016
Manuscript under review for journal Earth Surf. Dynam.
Published: 28 June 2016

$$\overline{w'^2}^{+}(z^{+}) = 1.2 - \frac{1.2}{85^3}(90 - z^{+})^3 \qquad (9)$$

Equation (9) has been plotted as the red line in Figure 2. The agreement between Eq. (9), DNS data, and measurements is strong. The numerical values in Eq. (9) are the result of the fit to the boundary conditions at $z^{+}=5$ and $z^{+}=90$, the agreement of the shape of Eq. (9) and the observed universal distribution of $\overline{w'^2}^{+}$ justifies the functional form assumed *a priori* in Eq. (7).

The present aim is to compare turbulent forces between $5<z^{+}<90$ to gravity acting on the suspended sediment. The average non-dimensional acceleration between $5<z^{+}<90$ is evaluated from Eq. (7) as

$$\left\langle \overline{a}^{+} \right\rangle_{5}^{90} = \frac{1.2}{170} \qquad (10)$$

Which, in combination with Eq. (6) yields

$$\left\langle \overline{a} \right\rangle = \frac{1.2u^{*3}}{170\nu} \qquad (11)$$

F_{turb} is now obtained by the Newtonian inference that the upwards acceleration is the expression of a net upward turbulent force acting per unit volume of fluid:

$$F_{turb} = \rho_f \left\langle \overline{a} \right\rangle = \frac{1.2\rho_f u_*^3}{170\nu}. \qquad (12)$$

We now introduce the non-dimensional near-boundary suspension capacity parameter Γ to compare the vertical turbulent forces to the gravity force acting on suspended particles per unit volume F_g.

$$\Gamma = \frac{F_{turb}}{F_g} = \frac{\rho_f \ 1.2u_*^3}{170\nu g\left(\rho_s - \rho_f\right)C_b} = \frac{u_*^3}{140\nu g R C_b}, \qquad (13)$$

with $R = \rho_f / (\rho_s - \rho_f)$ being the relative density of sediment submerged in water. The numerical constant 140 derives from the scales of vertical turbulence discussed above [1.2/(2*(90-5))], and the propagated uncertainty from the estimation of turbulent scales from measurement is +/-20.

2.2 Interpretation

The absence of particle size d from Eq. (13) is a strong breach of the established intuition that grainsize is a primary control on particle suspension. The proposal of Eq. (13) is therefore a strong argument for a capacity perspective of particle

Earth Surf. Dynam. Discuss., doi:10.5194/esurf-2016-33, 2016
Manuscript under review for journal Earth Surf. Dynam.
Published: 28 June 2016

suspension, as opposed to a competence perspective [*Hiscott*, 1994; *Dorrell et al.*, 2013]. Of course the dichotomy cannot be complete, and the role of grainsize in limiting the suspended particle concentration will be discussed in Section 4, following the interpretation and discussion of the primary structure of the suspension capacity parameter.

When $\Gamma>1$ the average vertical turbulent force in the flow exceeds the gravitational pull on the suspended particles, the suspension is under-saturated. Such conditions might arise from a lack of availability of particles to suspended, either due to an absence of particles on the wall, due to particle size inhibiting entrainment from the wall, or due to cohesive forces keeping particles attached to the wall. The turbulent force F_{turb} has been estimated from clear water turbulence kinematics above. This clear water turbulent force can be interpreted as a force budget that is available to either accelerate fluid or support particles in suspension. This interpretation leads to the prediction that vertical turbulent kinematics are suppressed in the presence of suspended particles at concentrations below the saturation concentration, since only part of the turbulent force budget remains to establish the vertical accelerations. The direct numerical simulations of turbulent flows with suspended particles by Cantero and co-workers demonstrate that turbulence intensity near the boundary of the flow is decreased in the presence of particles for all components (u,v,w) at under-saturation [*Cantero et al.*, 2009]. This decrease in the statistical intensity of turbulence is linked to the decreased occurrence of hairpin vortices in those simulations [*Cantero et al.*, 2009].

At $\Gamma=1$, turbulent forces in the near wall region of the flow are in equilibrium with the gravitational pull on the suspended particle load, this force balance prevents average net vertical acceleration of the sediment particles and the fluid between them. The flow is precisely saturated with suspended sediment near the boundary and C_b can be seen as a saturation concentration. Equation (13) can thus be used as an analytical expression for near wall equilibrium concentration when Γ is set to 1. Graf and Cellino [2002] report turbulence intensities measured in the presence of suspended sediment at saturation. Turbulence intensities of both vertical and streamwise components are reported to be suppressed close to the boundary of their experiments. It is suggested here that turbulence becomes completely suppressed at saturation, though the experimental techniques of Graf and Cellino did not allow confident assessment of turbulence at $z^+<90$.

When $\Gamma<1$, gravitational pull on the sediment dominates, and the flow does not have sufficient capacity to suspend all the particles present in the near-boundary region. The flow is over-saturated with sediment. This situation can be regarded from a particle perspective and a continuum perspective, both resulting in deposition of sediment from the base of the flow: firstly, from a particle perspective, particles will, on average, experience a wall-bound gravitational body force that exceeds turbulent pressure and viscous forces acting on the particle surfaces, and they will accelerate towards and settle onto the boundary; secondly, from the continuum perspective of the turbulent flow, the upward turbulent pressure and viscous forces are smaller than downward gravitational forces applied to the fluid by the particles, this prevents turbulent accelerations and results in turbulence extinction. Turbulence extinction at over-saturation must be expected to result in sedimentation as there is no mechanism countering gravitational settling of sediment. This second perspective is reminiscent of a recent breakthrough in DNS simulations of suspension flows [*Cantero et al.*, 2009, 2011, 2012] that demonstrates how turbulence at the base of suspension flows is rapidly extinguished in over-saturated suspensions. The studies by Cantero and co-workers

Earth Surf. Dynam. Discuss., doi:10.5194/esurf-2016-33, 2016
Manuscript under review for journal Earth Surf. Dynam.
Published: 28 June 2016

demonstrate that complete suppression of turbulence at oversaturation is related to the disappearance of the streak-vortices that form the legs of hairpin-vortices. These hairpin vortices are the dominant vertical structures in near-boundary turbulence [*Smith, C. R and Walker*, 1995; *Zhou et al.*, 1999; *Adrian*, 2007], and their legs normally occupy the zone between $5<z^+<90$. Their suppression signifies a complete shutdown of the production of near-boundary turbulence, leading to rapid laminarization extending far beyond the normal viscous sublayer thickness.

3 Comparisson of Γ to measurements and previous formulations

3.1 Measurements

Γ=1 for quartz particles in water at 10° C is plotted in Figure 3a, together with measurements of suspended particle concentrations. The graph supports the notion that any suspension flow with a suspension capacity parameter smaller than 1, which corresponds to the region above the Γ=1 iso-line in Figure 3, results in rapid deposition from the base of the flow, and a return to capacity transport. Data from studies with saturated suspensions [*Smith and McLean*, 1977; *Coleman*, 1986; *Bennett et al.*, 1998; *Graf and Cellino*, 2002; *Cartigny et al.*, 2013] lie around Γ=1.

Γ=1 also envelopes the upper range of data points from Vanoni [1940], Einstein and Chien [1955], Ordoñez [1970], and Montes [1973]. These measurements represent under-saturated suspensions in experiments where the flume floor consisted of smooth-glass or was covered by glued down sand-particles. Both conditions avoided formation of loose granular beds. Therefore, "it is doubtful if enough material was ever available to completely load the flow" [*Vanoni*, 1940].

3.2 Previous formulations

The turbulence extinction threshold (— , Figure 3b, [*Cantero et al.*, 2009, 2011, 2012]) is virtually identical to Γ=1. The simple form of Eq. (13) has major advantages, however, over the threshold proposed by Cantero et al., which necessitates parameterizations using flow depth, sediment grainsize and settling velocity, and has bulk-flow-Reynolds-scale dependency. Appendix A contains details on choices made for the parameterization of Cantero et al.'s threshold condition in Figure 3b. The close correspondence with Γ=1 indicates that the here proposed force balance of the suspension capacity captures the mechanism of the underlying full suppression of hairpin-vortex turbulence generation observed in DNS experiments [*Cantero et al.*, 2009, 2011, 2012].

It has not been previously resolved whether the physically appropriate boundary condition of a suspension field should be a summation of the inward and outward fluxes through the boundary, or a boundary concentration. Many multiphase modelling approaches define a sedimentation flux towards the flow boundary dependent on sediment concentration and the stagnant-water terminal settling-velocity w_s; and an entrainment flux away from the flow boundary that is empirically related to flow conditions. Such flux-based equilibrium can be compared directly to the near-bed saturation concentration in the phase space of Figure 3; which is illustrated by equating the sedimentation flux to an often-used empiric entrainment flux [*Garcia and Parker*, 1991, 1993]

Earth Surf. Dynam. Discuss., doi:10.5194/esurf-2016-33, 2016
Manuscript under review for journal Earth Surf. Dynam.
Published: 28 June 2016

$$C_b w_s = \frac{AZ^5}{1+\frac{AZ^5}{0.3}} w_s, \quad (14)$$

where A is an empiric constant and Z empirically depends on u^*, particle size and density, and fluid density and viscosity. The empiric flux-based approach is similar to the present saturation concentration theory (Figure 3b).

Empiric relations have been used as closures for suspension concentration fields in sediment transport budget calculations in the absence of theory. Figure 3c compares the present theory with a number of proposed formulations, for the case of 150 μm sand (see Appendix A for details of these formulations and the parameterizations used). The empiric relations have a similar general signature as the theory, but the capacity theory outperforms the previous relations when the predictions of measurements is considered (Figure 3c).

4 Particle size

Particle size d is often regarded as a main control on particle suspension because larger particles settle faster under action of gravity. This leads to an intuitive incorporation of the settling velocity w_s in assessment of particle suspension transport, mostly in a non-dimensional ratio with the friction velocity following Bagnold [1966], or in the non-dimensional Rouse number following Rouse [1937]. This intuitive approach is not satisfactory in the near-boundary zone where terminal settling velocities in stagnant water cannot be justified to be the main controlling parameter as turbulent structures of the size of particles are associated with turbulent accelerations that may exceed g [*Irmay*, 1960; *Bagnold*, 1966; *La Porta et al.*, 2001]. Also, note how w_s is immediately dropped from Eq. (14) to yield a balance between erosion and deposition that relates the basal concentration to the friction velocity, quantitatively approaching Γ=1 (Figure 3b). The Stokes number, rather than the Rouse number, is an appropriate measure for the differential motion between particles and turbulent structures. The Stokes number is the non-dimensional ratio of particle relaxation time and a characteristic hydrodynamic timescale. The particle relaxation time is

$$T_{particle} = \frac{\rho_s d^2}{18\rho_f \nu}. \quad (15)$$

The characteristic timescale of the hydrodynamic setting at hand is determined from the equations of motion of the fictitious average parcel in the near boundary region. The timescale for the acceleration of the fictituous average parcel is used as the hydrodynamic timescale:

$$T_{hydrodynamic} = \frac{\Delta w'^{+}_{RMS}}{\left\langle \overline{a} \right\rangle} = \frac{170\nu}{\sqrt{1.2}u^{*2}}, \quad (16)$$

and the Stokes number for the problem at hand is

Earth Surf. Dynam. Discuss., doi:10.5194/esurf-2016-33, 2016
Manuscript under review for journal Earth Surf. Dynam.
Published: 28 June 2016

$$St = \frac{\rho_s d^2}{18\rho_f \nu} \Big/ \frac{170\nu}{\sqrt{1.2}\, u^{*2}}. \qquad (17)$$

Particles with St<<1 are responsive to viscous forces exerted by the surrounding fluid, tend to follow turbulent movements of the fluid parcels in the near boundary region, and will attain saturation concentrations predicted by Γ=1 irrespective of their grain size. Trajectories of larger particles with St>1 will not mimic the fluid flow path and behave ballistically. Such ballistic behavior will cause a lag both in acceleration away from the bed in upward turbulent excursions and deceleration in downward turbulent excursions. The former will result in entrainment limited suspension, the latter in enhanced deposition, and both cause concentrations of larger particles to be below the predictions of Γ=1. Figure 4 displays the Stokes number for quartz particles of different sizes in the silt to fine-grained-sand classes. Particles of d<250 μm have St<1 in water for the range of friction velocities (u*<0.15) typically encountered in natural flows. The implication is that particle size has no first order effect on suspension capacity for quartz particles smaller than 250 μm in water.

5 Discussion and conclusions

We have introduced a non-dimensional suspension capacity parameter Γ, which compares the gravity forces acting on the near-bed suspended particles to the vertical turbulent force acting near the base of a turbulent flow. Γ is general for particles in a turbulent viscous fluid near a boundary, and while focus here is on applications to water-born transport of natural sediment particles near the base of rivers and above the seafloor, it can be applied to a wide variety of multiphase transport problems in terrestrial and extraterrestrial flows. It needs only be applied to regions within flows where turbulent stress gradients are large. In many problems, this region extends only a few millimeters from the flow boundary, and the present theory is therefore especially useful as concentration boundary condition at flow boundaries in simulations. Dynamic suspension support by turbulent stress gradients can generally be neglected in the bulk of the turbulent fluid, because turbulent stress gradients are much smaller above the turbulence intensity maximum (Figure 2); there, dispersion modelling using drift-velocity or drag approaches [*McTigue*, 1981; *Basani et al.*, 2014], or the Rouse number suffice. Figures 3b-c yield justification for model simulations utilizing Eq. (14) or other empiric closures [*Smith and McLean*, 1977; *van Rijn*, 1984; *Garcia and Parker*, 1991, 1993; *Zyserman and Fredsoe*, 1994] for the near-wall boundary condition, but it is suggested here that a saturation concentration C_b calculated with the suspension capacity parameter Γ=1 can be used as an appropriate boundary condition in future work. The suspension capacity parameter Eq. (13) does more justice to available concentration measurements, and eliminates the need to set values of non-physical empiric parameters.

Particle size is absent from the suspension capacity parameter, but it does appear in the Stokes number. Large particles with St>>1 will start to behave ballistically and travel straight through turbulent eddies without following the turbulent accelerations of the fluid. The concentration of such ballistic particles must be expected to be lower than the C_b predicted for Γ=1. St is lower than 1 for clay, silt, and very-fine- and fine-grained sediment particles in water, under all reasonable

Earth Surf. Dynam. Discuss., doi:10.5194/esurf-2016-33, 2016
Manuscript under review for journal Earth Surf. Dynam.
Published: 28 June 2016

turbulent conditions (Figure 4). This means that for the vast majority of sediment, grainsize bears no influence on how much sediment can be transported in suspension by water close to the Earth's surface.

Gravitational acceleration g is absent from St, as particle size d is absent from Γ. Therefore, gravity and particle size are not combined in either of the two non-dimensional groupings that determine the suspension capacity and particle-size dependence of suspension. This must mean that the kinematic scale of settling velocity under gravity w_s is an irrelevant variable for the problem of turbulent suspension capacity in the near-wall region.

Appendix A Previously proposed empirical relations for the near boundary particle concentration

A.1 Cantero et al. (2009, 2011. 2012)

Cantero et al. [2009, 2011, 2012] have empirically determined a threshold above which turbulence in flows at the base of their DNS experiments is fully suppressed

$$\frac{\mathrm{Ri}_\tau \widetilde{w_s}}{\mathrm{K_c}\{\mathrm{Re}_\tau\}} = 1 \frac{Ri_\tau \widetilde{w_s}}{\mathcal{K}_c\left\{Re_\tau\right\}} = 1 \,, \tag{A.1.1}$$

where the subscript τ denotes the shear-Richardson and shear-Reynolds flow scales, defined as

$$Ri_\tau = \frac{g\left(\rho_s/\rho_f - 1\right)CH}{u^{*2}} \text{, and } Re_\tau = \frac{u^* H}{\nu} \,, \tag{A.1.2}$$

where C is the average sediment concentration, and H the flow size perpendicular to the wall. The settling velocity w_s has been made non-dimensional by

$$\widetilde{w_s} = \frac{w_s}{u^*} \,. \tag{A.1.3}$$

And the weak dependence of the turbulence threshold value on the Reynolds number is suggested to be [*Cantero et al.*, 2012]

$$\mathcal{K}_c = 0.041 \ln\left(Re_\tau\right) + 0.11 \,. \tag{A.1.4}$$

The term $Ri_\tau \widetilde{w_s}$ has a structure that is very similar to $1/\Gamma$:

$$Ri_\tau \widetilde{w_s} = \frac{g\left(\rho_s - \rho_f\right)CHw_s}{\rho_f u^{*3}} \tag{A.1.5}$$

This means that a direct comparison between Γ and the turbulence suppression in DNS is possible when the turbulence extinction threshold is parameterized with appropriate values for H and w_s. The plotted line in Figure 3b has been parameterized with the scales of the experimental comparison proposed in Table 2 of Cantero et al. [2012]. The ratio of near-

Earth Surf. Dynam. Discuss., doi:10.5194/esurf-2016-33, 2016
Manuscript under review for journal Earth Surf. Dynam.
Published: 28 June 2016

boundary concentration and depth-averaged concentration at turbulence suppression has been set to 3.45 in accordance to Figure 1 of Cantero et al. [2012].

A.2 Smith and McLean (1977)

Smith and McLean [1977] suggest

$$C_b = \frac{C_{max}\gamma_0 T}{\left(1+\gamma_0 T\right)} \qquad \text{(A.2.1)}$$

for the functional form for the sediment concentration at the reference level, where C_{max} is the maximum sediment concentration, T is the transport stage parameter [*van Rijn*, 1984, 1993], and γ_0 is an empirical constant O(10^{-3}). Choices for the appropriate values of these parameters have been made so as to follow the original publication [*Smith and McLean*, 1977]. C_{max} is set to 0.65 [*Smith and McLean*, 1977]. The claimed appropriate value for γ_0 varies; the original publication reports fitted and computed values between 1.9 and 2.4, while a value of 4 is also reported [*van Rijn*, 1993]. Here, the original concentration measurements for 270 μm sand are used to calculate the value of γ_0 that makes Eq. (A.2.1) satisfy each original measurement individually:

γ_0 = [0.0033; 0.0087; 0.0034; 0.0037; 0.0030; 0.0030; 0.0030].

The average value is 4.0e-3, and this is used in Figure 3c.

A.3 Zyserman and Fredsøe (1994)

Zyserman and Fredsøe [1994] suggested

$$C_b = \frac{A\left(\theta-\theta_{cr}\right)^n}{1+\dfrac{A\left(\theta-\theta_{cr}\right)^n}{c_m}} \qquad \text{(A.3.1)}$$

as an empiric relation between suspended particle concentration and flow conditions, where θ is the Shields parameter. The critical Shields parameter θ_{cr} has been calculated with an explicit analytical formulation [*Cao et al.*, 2006]. The value of the empiric parameters as suggested in the original publication [*Zyserman and Fredsøe*, 1994] are used in Figure 3c: A=0.331; n=1.75; and c_m=0.46.

A.4 van Rijn (1984)

van Rijn [1984] suggested for the near boundary particle concentration

$$C_b = \frac{0.035 d T^n}{\alpha_2 z_a d^{*m}}, \qquad \text{(A.4.1)}$$

where d is the median particle size, and * denotes a non-dimensionalisation with viscosity, density and gravity scales. The empiric constant and exponents are here used as suggested in the original publication [*van Rijn*, 1984]: α_2=2.3; n=1.75; and m=0.3. A number of different ways have been proposed to set the elevation of the reference level z_a, the elevation of z^+=*90* is used here.

6 Acknowledgements

This is Kavli Institute of Theoretical Physics at UCSB report ####, supported in part by the National Science Foundation (grant# NSF PHY11-25915). JTE acknowledges the organisers and attendees of KITP GeoFlows2013 and the Max Planck Institute for Physics of Complex Systems GeoFlows2016 for discussions. This contribution is part of the Eurotank Studies of Experimental Deepwater Sedimentology (EuroSEDS), supported by the Netherlands Organisation for Scientific Research (grant# NWO 864.13.006), ExxonMobil, Shell, and Statoil.

References

Adrian, R. J. (2007), Hairpin vortex organization in wall turbulence, *Phys. Fluids*, *19*, 041301, doi:10.1063/1.2717527.

Bagnold, R. A. (1966), *Bagnold_1966_ Sediment Transport from general Physics.pdf*, Washington.

Basani, R., M. Janocko, M. J. B. Cartigny, W. M. Hansen, and J. T. Eggenhuisen (2014), MassFLOW-3D TM as a simulation tool for turbidity currents : some preliminary results, *IAS Speical Publ.*, *46*, 587–608, doi:10.1002/9781118920435.ch20.

Bennett, S. J., J. S. Bridge, and J. L. Best (1998), Fluid and sediment dynamics of upper stage plane beds, *J. Geophys. Res.*, *103*(C1), 1239–1274.

Cantero, M. I., S. Balachandar, and G. Parker (2009), Direct numerical simulation of stratification effects in a sediment-laden turbulent channel flow, *J. Turbul.*, *10*(December 2013), 37–41, doi:10.1080/14685240903159197.

Cantero, M. I., A. Cantelli, C. Pirmez, S. Balachandar, D. Mohrig, T. a. Hickson, T. Yeh, H. Naruse, and G. Parker (2011), Emplacement of massive turbidites linked to extinction of turbulence in turbidity currents, *Nat. Geosci.*, *5*(1), 42–45, doi:10.1038/ngeo1320.

Cantero, M. I., M. Shringarpure, and S. Balachandar (2012), Towards a universal criteria for turbulence suppression in dilute turbidity currents with non-cohesive sediments, *Geophys. Res. Lett.*, *39*(May), L14603, doi:10.1029/2012GL052514.

Cao, Z., G. Pender, and J. Meng, (2006), Explicit formulation of the Shields diagram for incipient motion of sediment, J. Hydraul. Eng., 132, 1097-1099, doi: 10.1061/(ASCE)0733-9429(2006)132:10(1097).

Cartigny, M. J. B., J. T. Eggenhuisen, E. W. M. Hansen, and G. Postma (2013), Concentration-Dependent Flow Stratification In Experimental High-Density Turbidity Currents and Their Relevance To Turbidite Facies Models, *J.*

Sediment. Res., *83* (12), 1047–1065, doi:10.2110/jsr.2013.71.

Coleman, N. L. (1986), Effects of Suspended Sediment on the Open-Channel Velocity Distribution, *Water Resour. Res.*, *22*(10), 1377, doi:10.1029/WR022i010p01377.

Day, M. A. (1990), The no-slip condition of fluid dynamics, *Erkenntnis*, *33*(3), 285–296, doi:10.1007/BF00717588.

Dorrell, R. M., A. J. Hogg, and D. Pritchard (2013), Polydisperse suspensions : Erosion , deposition , and flow capacity, *J. Geophys. Res. Surf.*, *118*(August), 1939–1955, doi:10.1002/jgrf.20129.

Dreeben, T. D., and S. B. Pope (1998), probability density function/Monte Carlo simulation of near-wall turbulent flows, *J. Fluid Mech.*, *357*, 141–166.

Garcia, M., and G. Parker (1991), Entrainment of bed sediment into suspension, *J. Hydraul. Eng.*, *117*(4), 414–435.

Garcia, M., and G. Parker (1993), Experiments on the entrainment of sediment into suspension by a dense bottom current, *J. Geophys. Res.*, *98*, 4793–4807, doi:10.1029/92JC02404.

De Graaff, D. B., and J. K. Eaton (2000), Reynolds-number scaling of the flat-plate turbulent boundary layer, *J. Fluid Mech.*, *422*, 319–346, doi:10.1017/S0022112000001713.

Graf, W. H., and M. Cellino (2002), Suspension flows in open channels ; experimental study, *J. Hydraul. Res.*, *40*(4), 435–447.

Grass, A. J. (1971), Structural features of turbulent flow over smooth and rough boundaries, *J. Fluid Mech.*, *50*, 233–255, doi:10.1017/S0022112071002556.

Hiscott, R. N. (1994), Loss of capacity, not competence, as the fundamental process governing deposition from turbidity currents, *J. Sediment. Res.*, (3), 209–214.

Irmay, S. (1960), Accelerations and mean trajectories in turbulent channel flow, *J. Basic Eng.*, 961–972.

Leeder, M. (1983), On the dynamics of sediment suspension by residual Reynolds stresses—confirmation of Bagnold's theory, *Sedimentology*, *30*, 485–491, doi:10.1111/j.1365-3091.1983.tb00687.x.

Leeder, M. R. (2007), New criterion for sediment suspension and wind-speed proxy in planetary atmospheres, *Geophys. Res. Lett.*, *34*(1), L01201, doi:10.1029/2006GL027051.

Leeder, M. R., T. E. Gray, and J. Alexander (2005), Sediment suspension dynamics and a new criterion for the maintenance of turbulent suspensions, *Sedimentology*, *52*(4), 683–691, doi:10.1111/j.1365-3091.2005.00720.x.

McTigue, D. F. (1981), Mixture theory for suspended sediment transport, *J. Hydraul. Div. Am. Soc. Civ. Eng.*, *107*, 659–673.

Montes Videla, J. S. (1973), Interaction of two dimensional turbulent flow with suspended particles,

Nezu, I., and H. Nagakawa (1993), *Turbulence in open channel flow*, Balkema, Rotterdam.

Pope, S. B. (2000), *Turbulent Flows*, Cambridge University Press, Cambridge.

La Porta, A., G. A. Voth, A. M. Crawford, J. Alexander, and E. Bodenschatz (2001), Fluid particle accelerations in fully developed turbulence, *Nature*, *970*(1), 1017–1019.

van Rijn, L. C. (1984), Sediment transport, ppart II: Suspended load transport, *J. Hydraul. Eng.*, *110*(11), 1613–1641.

van Rijn, L.C. (1993), Principles Of Sediment Transport In Rivers, Estuaries And Coastal Seas, Aqua publications, Amsterdam, the Netherlands.

Rouse, H. (1937), Modern conceptions of the mechanics of turbulence, *Trans. Am. Soc. Cicvil Eng.*, *102*(1), 463–505.

Smith, C. R, and J. D. A. Walker (1995), Turbulent wall layer vortices, in *Fluid vortices*, edited by S. I. Green, pp. 235–290, Kluwer Academic.

Smith, J. D., and S. R. McLean (1977), Spatially averaged flow over a wavy surface, *J. Geophys. Res.*, *82*(12), 1735, doi:10.1029/JC082i012p01735.

Spalart, P. R. (1988), Direct simulation of a turbulent boundary layer up to Re-theta= 1410, *J. Fluid Mech.*, *187*(December), 61–98.

Stokes, G. G. (1851), On the Effect of the Internal Friction of Fluids on the Motion of Pendulums, *Trans. Cambridge Philos. Soc.*, *9*, 8, doi:10.1017/CBO9780511702242.005.

Townsend, A. A. (1976), *The structure of turbulent shear flow*, 2nd ed., Cambridge University Press, New York.

Vanoni, V. A. (1940), Experiments on the transportation of suspended sediment by water, , 80.

Vedula, P., and P. K. Yeung (1999), Similarity scaling of acceleration and pressure statistics in numerical simulations of isotropic turbulence, *Phys. Fluids*, *11*(5), 1208–1220.

Yeo, K., B. G. Kim, and C. Lee (2010), On the near-wall characteristics of acceleration in turbulence, *J. Fluid Mech.*, *659*, 405–419, doi:10.1017/S0022112010002557.

Zhou, J., R. J. Adrian, S. Balachandar, and T. M. Kendall (1999), Mechanisms for generating coherent packets of hairpin vortices in channel flow, *J. Fluid Mech.*, *387*, 353–396, doi:10.1017/S002211209900467X.

Zyserman, J. A., and J. Fredsoe (1994), Data analysis of bed concentration of suspended sediment, *J. Hydraul. Eng.*, *120*(9), 1021–1042.

Earth Surf. Dynam. Discuss., doi:10.5194/esurf-2016-33, 2016
Manuscript under review for journal Earth Surf. Dynam.
Published: 28 June 2016

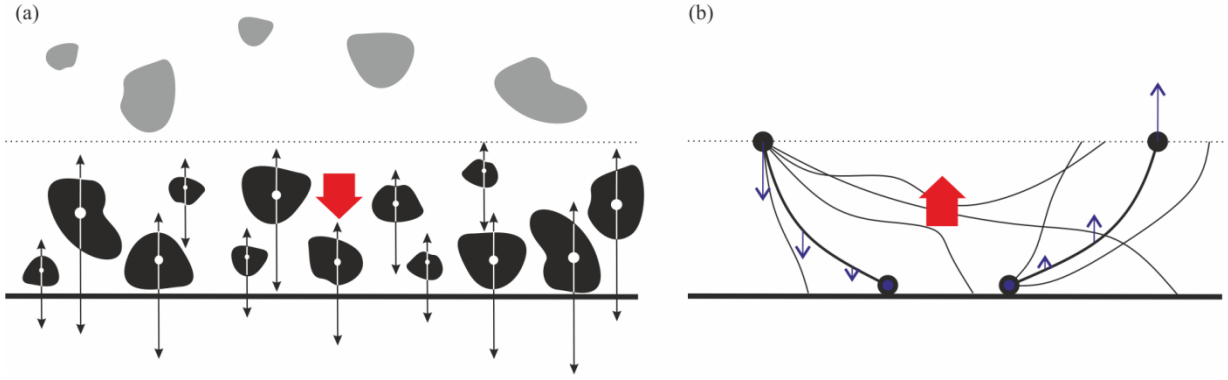

Figure 1. Schematic diagram of gravity and turbulence acting on the suspension within the near-boundary region.(a) Each particle is acted upon by a downward-directed gravitational force and upward directed buoyancy force (black arrows). Particles in suspension above the near-boundary region, indicated in grey, are not considered herein. The red arrow indicates F_g acting on the suspended particle load within the near-boundary region. (b) The vertical turbulent velocity *w'* (blue arrows) is 0 m/s at the impermeable no-slip boundary at the base of the suspension, and increases throughout the near-boundary region. Parcels of suspension moving upwards or downwards through the top of the near-boundary region are subject to a multitude of possible velocity evolutions (thin black lines), which can be represented by the pathways of "fictitious average parcels" (thick black lines; [*Irmay*, 1960]). The blue arrows indicate the vertical component of velocity; parcels with decreasing downwards velocities and increasing upwards velocities both experience upwards acceleration. The red arrow indicates F_{turb} derived from this average upwards fluid acceleration.

Earth Surf. Dynam. Discuss., doi:10.5194/esurf-2016-33, 2016
Manuscript under review for journal Earth Surf. Dynam.
Published: 28 June 2016

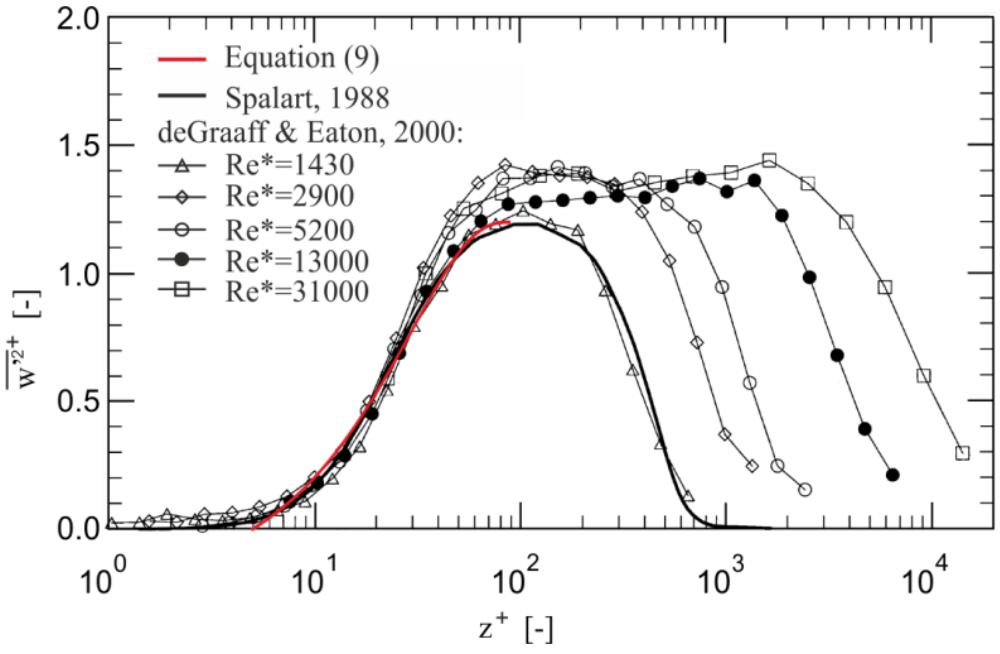

Figure 2. Equation 9 compared to universal scaling of the vertical turbulent velocity in the near-boundary region in DNS [Spalart, 1988] and physical experiments [De Graaff and Eaton, 2000]. Equation (9) is plotted as a red line. Modified after [De Graaff and Eaton, 2000].

5

Earth Surf. Dynam. Discuss., doi:10.5194/esurf-2016-33, 2016
Manuscript under review for journal Earth Surf. Dynam.
Published: 28 June 2016

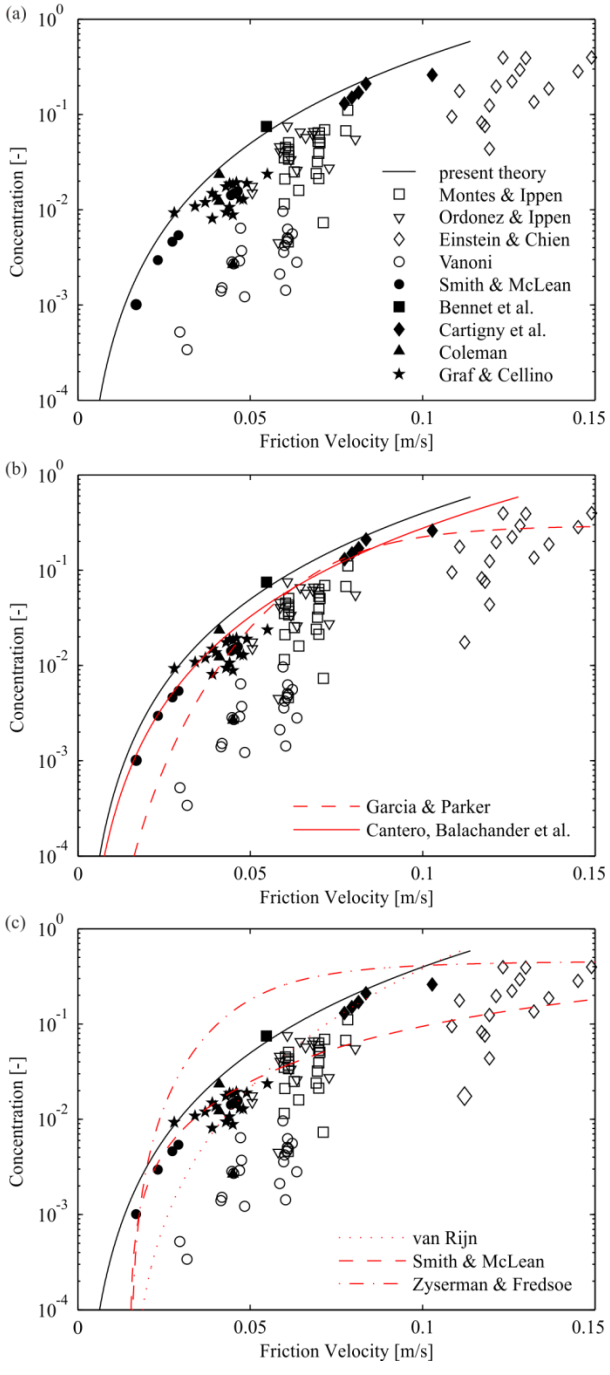

Figure 3. The suspension parameter for saturated suspensions (Γ=1) plotted in the space defined by the friction velocity and the near-boundary particle concentration. (a) Comparison of theory to measurements of saturated suspensions and measurements of under-saturated suspensions. (b) Comparison of theory to a threshold for turbulence extinction observed in DNS experiments [*Cantero et al.*, 2009, 2012a, 2012b], and balanced sedimentation-entrainment fluxes [*Garcia and Parker*, 1993]. (c) Comparison of theory to suggested empiric relations.

Earth Surf. Dynam. Discuss., doi:10.5194/esurf-2016-33, 2016
Manuscript under review for journal Earth Surf. Dynam.
Published: 28 June 2016

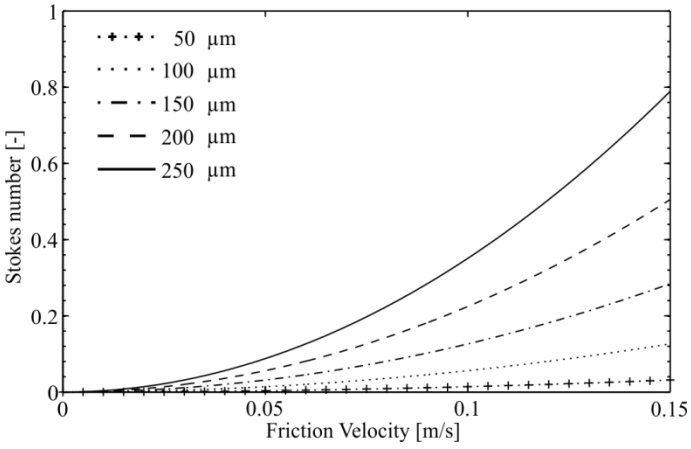

Figure 4. The Stokes number (Eq. 17) of different sized quartz particles in the near-boundary region.